# Dynamical properties of $LiI \cdot D_2O$. II. Vibrational modes and disordering effects

P. Migliardo and G. F. Romano
*Istituto di Fisica dell'Universitá and Centro Interuniversitario di Struttura della Materia and Gruppo Nazionale di Struttura della Materia del Consiglio Nazionale delle Ricerche, Via Dei Verdi, 98100 Messina, Italy*

F. Aliotta, A. Bartolotta, and G. Di Marco
*Istituto di Tecniche Spettroscopiche del Consiglio Nazionale delle Ricerche, Via Dei Verdi, 98100 Messina, Italy*
(Received 4 August 1986; revised manuscript received 25 February 1987)

The vibrational dynamics of $\alpha$-phase lithium iodide monodeuterate (LID) is investigated by Raman scattering as a function of temperature. A simple model is presented in order to explain the linkage between the $D_2O$ reorientation and the $Li^+$ hopping motion in the superionic $\alpha$ form. The internal O—D stretching and $D_2O$ bending regions are analyzed, within this model, by a suitable deconvolution of the symmetric lines. Spectral contributions that might originate from two possible polarization states of the $D_2O$ molecule are discovered. Raman spectra of the melt, both in the polarized (VV) and depolarized (VH) geometries, are also presented. The experimental data reveal that the melt, in spite of stronger anharmonicity effects, exhibits the same local order which is found in the $\alpha$ phase. Furthermore, a measurement performed at a fixed temperature ($T = -70\,^{\circ}C$) as a function of time shows a dependence of the spectral features on time, which confirms the existence of a structural phase transition towards an orthorhombic $\beta$ form, as also suggested by neutron diffraction data. The low-frequency translational region shows the characteristic broad features of a density of vibrational states both in the $\alpha$ phase and in the melt, thus confirming the highly cooperative nature of the dynamics of the system.

## I. INTRODUCTION

In the last few years, lithium iodide monodeuterate $LiI \cdot D_2O$ (LID) has been one of the most extensively studied solid electrolyte systems. Aside from its technological importance in the commercial development of solid-state batteries,[1,2] this system is interesting from a fundamental point of view because it represents a good model system for the study of disorder (both translational and rotational) effects in crystals.

The crystalline structure of LID is perovskitelike $I(H_2O) \cdot \frac{1}{3}Li_3$ ($\alpha$ phase). The unit cell is cubic (symmetry group $Pm3m$) having an iodine ion at each lattice site, whereas the lithium ions occupy only three of the fcc sites. As far as the water molecule is concerned the oxygen atom occupies approximately the bcc site[3] and the two O—D bonds point towards two opposite corners of a square face (see Fig. 4). A strong connection exists between the water orientation and the positions occupied by the lithium ions. In fact, in the equilibrium configuration, one of the lithium ions works as an electron-acceptor combination for the oxygen atom and stays on the $C_2$ axis where the O—$Li^+$ bond direction is opposite to the O—D $\cdots$ I directions, whereas the other two $Li^+$ ions have symmetric positions with respect to the water molecule plane. Consequently, 12 equivalent orientations for the water molecule exist and the two jumping lithium ions are distributed over size equivalent sites.[1,4] NMR measurements[4,5] yield almost the same values of relaxation times and activation energies both for lithium ions and protons, thus supporting the idea that there is a strong correlation between the hopping motion of lithium and the reorientation of the water molecule.

The superionic properties[6] of the $\alpha$- phase (stable from $-54\,^{\circ}C$ up to the melting temperature $T_m = +132\,^{\circ}C$) are connected to the existence of equivalent sites for the $Li^+$ ions. Recently a first-order phase transition ($T_c = -54\,^{\circ}C$) between the cubic and the orthorhombic $\beta$ forms ($Pmam$) was found (see Ref. 3 for details). In the ordered $\beta$ phase there are no more excess free sites for lithium ions and the superionic properties are lost. In a recent paper,[7] hereafter referred to as I, we studied the collective aspects of ionic dynamics by photon-correlation spectroscopy. The results, which are also connected to NMR spin-lattice relaxation data of $^7Li$, show a long relaxation time in the density fluctuation correlation function. A comparison between the correlation times $\langle \tau \rangle$ and the hopping times for lithium shows that these fluctuations are due to collective (translational and rotational) motions of clusters with a coherence length comparable to the wavelength of the probe. These correlated patches have been identified with $\beta$-phase domains inside the $\alpha$ structure, thus confirming the results obtained by diffuse elastic neutron scattering[3] and NMR (Ref. 4) measurements.

In order to obtain additional information about the very high-frequency dynamics of LID, we will present here an analysis of Raman scattering experiments performed over a wide temperature range. We have studied the Raman spectra both of the crystal and of the melt. We show that the water vibrational dynamics can be un-

 

derstood by means of a simple model connecting the reorientation of water molecules to the local hopping motions of lithium ions. The translational disorder of the system gives rise to a frequency distribution in the low-frequency ($\omega \leq 600$ cm$^{-1}$) region. Finally a comparison of the dynamical properties of the hydrated crystal with those of the melt seems to agree, for the latter, with a crystalike local order around the water molecule.

## II. EXPERIMENTAL PROCEDURE AND RESULTS

The Raman scattering measurements were performed on the same optically clear single crystal used for the NMR experiments (see Ref. 7 for details). The quartz cell, in which the cylindrical LID sample (deuterium isotopic purity of 99.996%) was sealed, was mounted in a homemade optical cryostat. The measurements were performed from $T=-58$ to 100 °C (in the $\alpha$ form), at $T=-70$ (below $T_c$) and at 142 °C (in the melt). In each run the temperature stability was better then 0.1 °C. We used a fully computerized triple monochromator manufacted by Spex (Ref. 8) that allowed us to collect data with a good signal-to-noise ratio starting within 9 cm$^{-1}$ of the Stokes shift. A 5145-Å exciting line was used from an $Ar^+$ Spectra-Physics laser with a mean power of 200 mW. For the $D_2O$ internal-mode regions (stretching and bending) we used a resolution of 2 cm$^{-1}$, and a resolution of 0.5 cm$^{-1}$ in the external modes region. Because of the highly hygroscopic nature of the LID single crystal, it was not possible to perform the usual analysis in order to determine the crystallographic axis. The only information available was that one of the crystalline axes coincided with the one of the cylindrical cell, which was oriented normally to the scattering plane. Consequently, we used a 90° scattering geometry without polarization analysis of the scattered light. $I_{VV}$ and $I_{VH}$ contributions were taken only for the molten crystal.

In Fig. 1 we report typical examples of Raman spectra for the crystalline $\alpha$ form ($T=-70$, $+25$, $+100$ °C) and molten ($T=142$ °C) LID in the 9 to 600 cm$^{-1}$ region of Stokes shift. In particular, for molten LID only the anisotropic contribution ($I_{VH}$) is shown, because the spectrum is fully depolarized over this frequency region. As expected, just an inspection of the figure shows a broadened distribution for both phases and this reflects strong anharmonic, disorder-induced effects in the system. In Figs. 2 and 3 the O—D stretching and bending spectra are shown for the crystal at different temperatures and the melt, respectively.

We shall now discuss the different spectral contributions within the framework of the current theories for the light scattering from disordered solids.

## III. DISCUSSION

In order to understand the nature of the LID Raman spectra, we need a description of the role played by the water molecule reorientation on the jumping lithium mechanism. Furthermore, we shall try to show the way the disorder in the arrangement of the lithium ions and in the $D_2O$ sublattices influences the vibrational dynamics of the system. Since the translational disorder in the $D_2O$ sublattice is induced by the random orientation of the water molecules, for the sake of clarity, we shall refer to it as "orientational disorder," throughout the rest of this article.

Bearing in mind the above points, we can expect a strong linkage effect between the local coordination and the dynamics. As far as the deuterium oxide is concerned, the units are arranged approximately on regular spatial positions (the center of the cube) but are oriented irregularly. This implies that the dipole moment changes from site to site depending on the direction assumed by the water molecule. In fact, we can think of the system as an electrically disordered lattice in which interaction-induced effects cause a time dependence of the derivative molecular polarizability tensor which induces a broad spectral distribution. In the literature, we find examples which show that the Raman scattering from disordered molecular crystals, such as $NH_4I$ (Ref. 9) and I*h* ice,[10] is successfully interpreted within such a framework.

The LID crystal, besides showing a reorientational

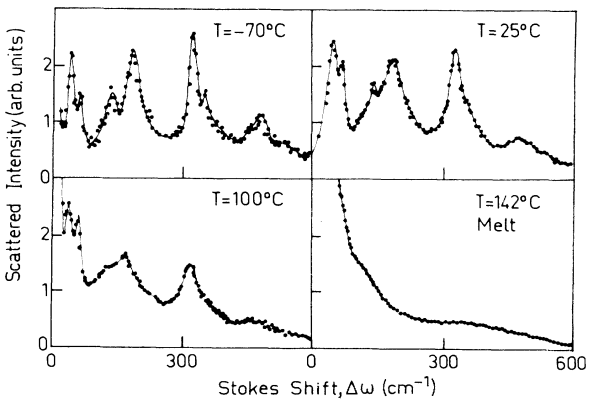


FIG. 1. Hindered translation region Raman spectra of the $\alpha$ phase of LID at three temperatures and of the melt. The continuous lines are guides for the eye.

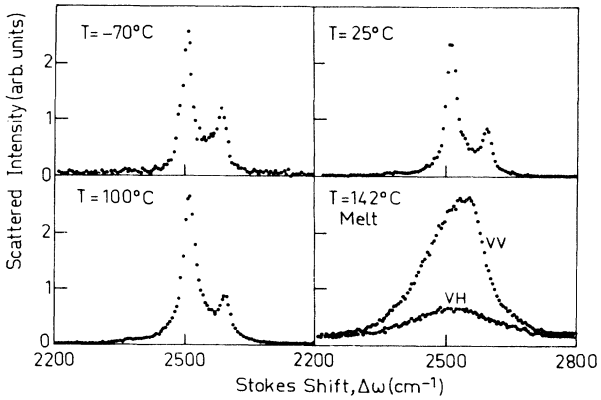


FIG. 2. Internal O—D stretching Raman spectra of the $\alpha$ phase of LID at three temperatures and of the melt.

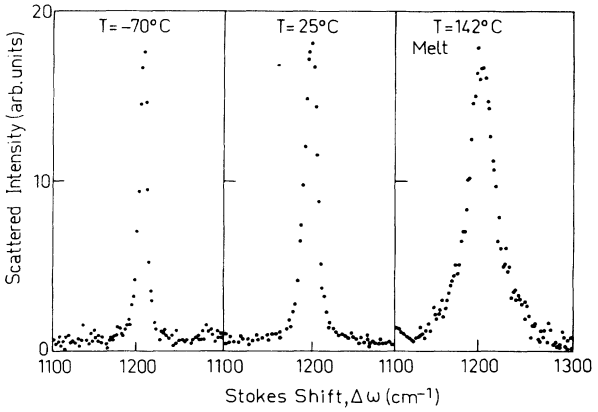


FIG. 3. Internal $D_2O$ bending Raman spectra of the $\alpha$ phase of LID at two temperatures and of the melt.

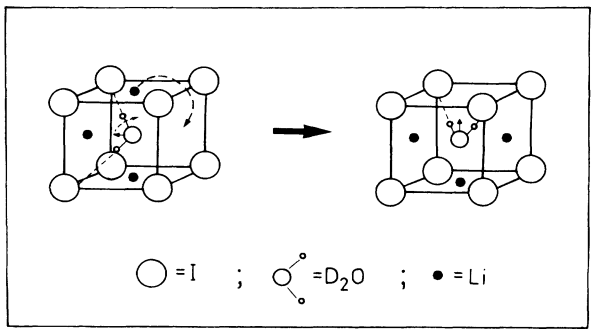


FIG. 4. Schematic view of the lithium ion jumping and of the water reorientation mechanisms.

disorder in the $D_2O$ molecules, because of its superionic properties, exhibits strong translational disorder even in the $Li^+$ sublattice. On looking at the "lattice" vibrations of the system, one finds that the "orientational" disorder of the stoichiometric $D_2O$ and the higher translational disorder in the $Li^+$ ions sublattice influences the low-frequency spectral region. Consequently, the system shows vibrational properties that are typical of disordered materials, and this trend has been shown for AgI, $RbAg_4I_5$, superionic crystals.[11] Due to the disorder, crystalline momentum selection rule is lost and the Raman spectra reflect the one-phonon vibrational density of states convoluted with the frequency dependent matrix elements.[12,13]

Since the cubic ells are the same (except for the water orientation) and the interaction of the $D_2O$ with the second neighbor ions is very weak, we can expect the orientational disorder to influence the internal modes of the molecule slight and, consequently, the usual phonon formalism can be applied. Therefore one might expect the Raman scattering to show the characteristic vibrational internal modes of the crystallization water in the cubic LID structure. The NMR relaxation time analysis that we performed in I allows us to assert that the $D_2O$ molecule (and the lithium ions) stay fixed within each unit cell until a structural breakup occurs. Before that breakup occurs and for a characteristic rest time, the $D_2O$ molecule undergoes a librational motion in the potential well as a result of the cation and anion binding forces. After a while, one can expect the local structure to evolve. We can assume a simple mechanism in which the jumping of one of the two lithium ions (which are not proton donors) occurs simultaneously with the breaking of one I · · · D bond. Consequently, we have a hindered rotation of the molecule around the intact I · · · D bond. This simple model is schematically sketched in Fig. 4. According to this model we must expect the reorientational mechanisms to be reflected in the internal $D_2O$ dynamics.

### A. The internal mode region

As far as the $D_2O$ internal vibrational modes are concerned, contributions arising from fully hydrogen bonded units (i.e., $D_2O$ in the local equilibrium position with $C_{2v}$ symmetry) should differ from contributions that originated from asymmetrically bonded molecules (reorienting $D_2O$ molecules having lower symmetry). However, it should be stressed that the above distinction is not to be taken quite literally. In fact, in our meaning, the latter occurrence includes all the polarization effects arising during the breaking and reforming of the I · · · D bond. The effects originated by the cation-water interaction were not taken into account because they affect only slightly the fundamental bending and stretching O—D modes.[14]

We have performed a suitable deconvolution[15] in symmetric (Lorentzian) lines of the spectra in the O—D stretching region. The result of such a computer calculation is shown as a solid line, in Fig. 5, for the spectrum at $T=25\,°C$. In the same figure, the deconvoluted bands are also shown. The two stronger bands centered at

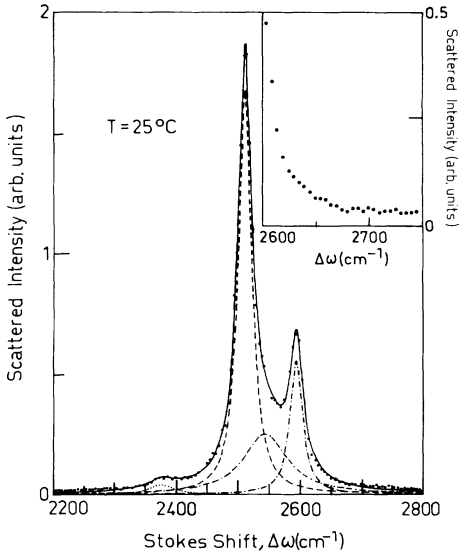


FIG. 5. O—D stretching Raman spectrum of the $\alpha$ crystal. Dots: experimental data. Solid line: best-fit result. Dashed lines: deconvoluted single Lorentzian lines. In the inset a magnified view of the spectrum between 2600 and 2750 $cm^{-1}$ is shown.

2512 and 2595 $cm^{-1}$ can be assigned to the total-symmetric and antisymmetric modes, respectively, of the water having the higher symmetry $C_{2v}$ (fully D-bonded $D_2O$). The above assignments are also consistent for hydrated crystals,[14] with the general spectroscopic observation that the stronger the hydrogen bond the lower the vibration frequency. Consequently the band centered at $\sim 2545$ $cm^{-1}$ having higher width and lower Raman intensity can be assigned to the total-symmetric vibration of the water that exhibits only one intact bond. The corresponding antisymmetric O-D mode should lie at a much higher frequency with very low intensity. The deconvolution procedure does not resolve, within the error limits, such a spectral contribution. Nevertheless, by looking at the inset of Fig. 5, it is possible to see a sharp slope variation of the wing of the band centered at $\sim 2595$ $cm^{-1}$, which suggests the presence of a spectral feature near 2636 $cm^{-1}$. Furthermore, a lower frequency shoulder exists ($\sim 2377$ $cm^{-1}$) that could be understood as originated by anharmonic effects[14,16,17] (i.e., a coupling between the $\nu_1$ mode of the $C_{2v}$ molecule with the $\sigma$ lattice motion $I \cdots D_2O$). In Fig. 6(a) the temperature evolution of the O—D stretching center frequencies is shown. The corresponding half widths at half maximum (HWHM) $\Gamma$ are shown as a function of $T$ in Fig. 6(b). The general trend of the lowering of the central frequencies when the temperature decreases is consistent with the fact that the binding energy increases at lower temperatures.[14,18] At the same time an increasing trend of the values with $T$ can be observed. In particular, strong anharmonicity effects can be detected by observing the absolute value of the variation as a function of $T$ of the antisymmetric mode of the fully D-bonded water. The values of the Lorentzian parameters $\Gamma$ and $\omega$ at the lowest temperature are worthy of comment. In order to test the dynamical effects of the $\alpha \rightarrow \beta$ phase transition (that occurs over a very long time, after the transition temperature is reached[3]), two consecutive Raman spectra at $T = -70$ °C were taken with a time interval of about 24 h. The results thus obtained, marked in Fig. 6 as solid circles and triangles, respectively, show that a clear spectral variation exists. This circumstance suggests that a phase transition is taking place, thus confirming the neutron scattering results.[3]

We next consider the $D_2O$ bending spectral contribution. In this case the deconvolution procedure yields two spectral contributions. In Fig. 7 the result of the fit and the two bands centered at $\sim 1196$ and 1203 $cm^{-1}$ are shown, as an example, for $T = 25$ °C. In the case of the D—O—D bending mode, the generally observed trend[14] is a shift to higher frequencies when the bond strength increases. Consequently, we can assign the band centered at $\sim 1203$ $cm^{-1}$ to the fully D-bonded water and the other to water having a lower symmetry. In Fig. 8 we present the results of a similar analysis on O—D stretching in molten LID, concerning the isotropic and anisotropic components. In this case the best fit shows spectral components which are easily recognizable in the corresponding $\alpha$ phase. As one expects, the higher values of each component reflect the fact that anharmonic effects play a major role in the internal modes of the melt. These results suggest that, even if the iodine cage loses its translational symmetry in the melt, it still exists as a local relaxing structure. In fact, we can think of molten LID as a hyperconcentrated electrolytic solution in which the cation and anion hydration shells[19,20,21] overlap thereby becoming the only hydration water for the system. Consequently, a local order occurs which is very similar to the one observed in the crystalline $\alpha$ form which gives rise to a similar dynamical response.

### B. The hindered translational region

We consider now the analysis of the spectral LID features in the low-frequency intermolecular translational region. As we have shown in Fig. 1 and on the basis of the arguments discussed above, the spectra are composed of rather broad overlapping components arising from the convolution of the density of states of the crystal with the electron phonon coupling functions.[12,13] Consequently, we have reduced our data by normalizing

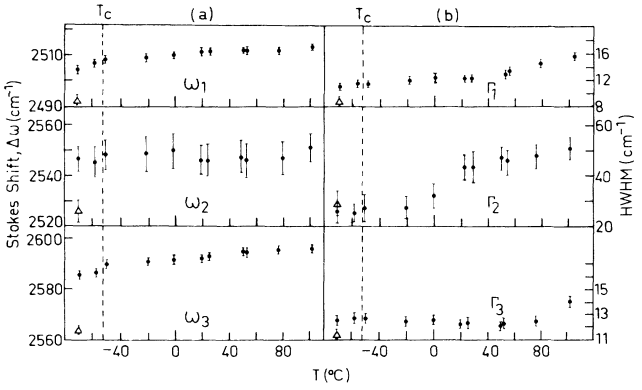


FIG. 6. Temperature dependence of the fitting Lorentzians parameteres. (a) Center frequencies $\omega$; (b) HWHM $\Gamma$. Triangles mark the results of the fitting of the experimental spectrum at $-70$ °C, that was taken 24 h after the thermostation was reached.

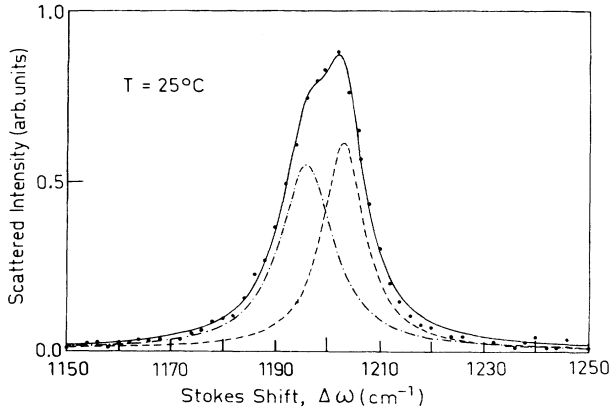


FIG. 7. O—D bending Raman spectrum at 25 °C of the $\alpha$ crystal. Dots: experimental data. Solid line: best-fit result. Dashed lines: deconvoluted single Lorentzian lines.

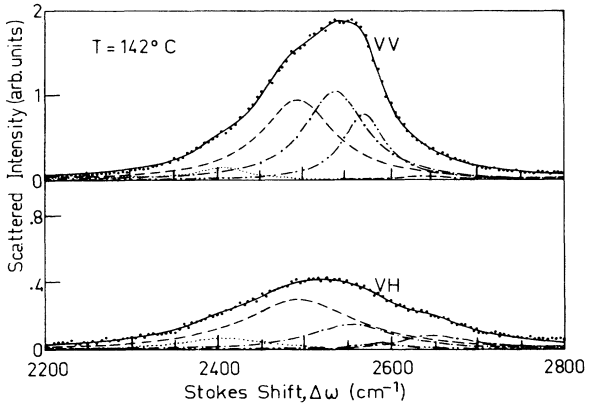


FIG. 8. O—D stretching Raman spectrum of the melt LID in the VV and VH scattering geometries. Dots: experimental data. Solid lines: best-fit results. Dashed lines: deconvoluted single Lorentzian lines.

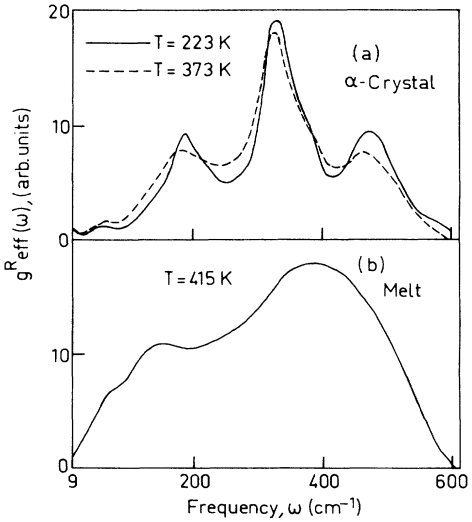


FIG. 9. Raman effective density of vibrational states. (a) $\alpha$ form at two temperatures; (b) melt.

them with the $\omega/[n(\omega,T)+1]$ Bose-Einstein population factor in the harmonic approximation.

The Raman effective density of states $g^R_{\rm eff}(\omega)$ given by

$$g^R_{\rm eff}(\omega)=I(\omega)\frac{\omega}{n(\omega,T)+1}=\sum_{\text{all bands } b} P^b(\omega)g_b(\omega) \qquad (1)$$

is then derived experimentally. In Eq. (1) the summation is extended over all of the $b$ bands; $P^b(\omega)$ are the Raman scattering matrix elements. In Fig. 9(a) the $g^R_{\rm eff}(\omega)$ for the crystal is shown at the extreme $\alpha$ phase temperatures. As Eq. (1) suggests, the resulting $g^R_{\rm eff}(\omega)$ is almost temperature independent. A similar data reduction has also been performed on molten LID. In this case the frequency distribution obtained [see Fig. 9(b)] also consists of broad features, that lie in the same frequency region as the corresponding $\alpha$ phase.

The relevant spectral components, for both the crystal and the melt, that appear in the 9 to 400 $cm^{-1}$, range, can be assigned to hindered ion-water bending and stretching. Furthermore, the broad band, centered at about 450 $cm^{-1}$ (resolved in the crystal), is due to the librational motion[22] of the water. By taking into account results of MD calculations[20,21] and Raman measurements[23,24] results on aqueous LiI solutions, it is possible to assign the $\sim$20 and 40 $cm^{-1}$ features to the I $\cdots$ D—O—D bond bending and the $\sim$170 and $\sim$190 $cm^{-1}$ contributions to the I $\cdots$ D—O—D bond stretching. The observed splitting agrees with our hypothesis that $D_2O$ exhibits two possible configurational states. Finally the spectral features, centered at $\sim$230 and 320 $cm^{-1}$, can be assigned to $Li^+$—O bending and stretching modes, respectively.

## IV. CONCLUDING REMARKS

In this paper we have studied the nature of the Raman spectra in a LID single crystal, as a function of temperature, in the superionic $\alpha$ phase. The light-scattering measurements were extended to the melt and the occurrence of the $\alpha \rightarrow \beta$ phase transition was also investigated. The Raman results agree very well with our starting hypothesis about the dynamics of the system. In fact, the data analysis allows us to draw the following conclusions.

(i) A close connection exists between the O-D internal vibrations and the local structure of the system. The crystallization water shows a rotational disordered that is strongly correlated with microscopic hoppings of the lithium ions. From a dynamical point of view, one can see the water developing a full hydrogen bond with the $I^-$ cage and, after a characteristic time, breaking one of the two bonds, thus allowing for reorientational motions. Consequently, the total-symmetric and antisymmetric O-D vibrational modes are split in pairs, which correspond to the two states. The $\alpha \rightarrow \beta$ phase transition was also tested by performing measurements as a function of time at fixed $T$, and a strong variation of the convoluted bands parameters was observed.

(ii) The high-frequency vibrational modes of the liquid phase show a close similarity with those of the $\alpha$ form, and this indicates that the same local order should exist in the two phases.

(iii) The low-frequency translational region, both for the $\alpha$ crystal and the melt, shows the characteristic very broad features of the one-phonon vibrational density of states. The various sub-bands were identified as deriving from the $Li^+$—O and I $\cdots$ D interactions.

Complementary measurements (ir and inelastic neutron scattering) are planned in order to confirm the highly cooperative nature of the LID dynamics.

## ACKNOWLEDGMENTS

The helpful scientific discussions with Professor M. Villa are gratefully acknowledged.

[1]K. Rudo, P. Hartwigi, and W. Weppner, Rev. Chim. Miner. **17**, 420 (1980).
[2]P. M. Skarstad, D. R. Merritt, and B. B. Owens, Solid State Ionics **3&4**, 277 (1981).
[3]N. H. Andersen, J. K. Kjems, and F. W. Poulsen, Phys. Scr. **25**, 780 (1982).
[4]J. L. Bjorkstam, M. Villa, M. Rahman, and P. M. Skarstad, Solid State Ionics **9&10**, 111 (1983).
[5]H. Chihara, T. Kawakami, and G. Soda, J. Magn. Res. **1**, 75 (1979).
[6]F. W. Poulsen, Solid State Ionics **2**, 53 (1981).
[7]A. Bartolotta, G. Di Marco, C. Vasi, P. Migliardo, and M. Villa, Phys. Rev. B **33**, 7481 (1986), and references therein.
[8]For the experimental details see, e.g., F. Aliotta, G. Maisano, N. Micali, P. Migliardo, C. Vasi, R. Triolo, and G. P. Smith, J. Chem. Phys. **76**, 3987 (1982).
[9]W. Dultz and H. Ihlefeld, J. Chem. Phys. **58**, 3365 (1973).
[10]G. Signorelli, V. Mazzacurati, M. Nardone, and C. Pona, in *Intermolecular Spectroscopy and Dinamical Properties of Dense Systems,* Proceedings of the International School of Physics "Enrico Fermi," Course LXXV (North-Holland, Amsterdam, 1980), pp. 294–306.
[11]See, e.g., S. Chandra, *Superionic Solids* (North-Holland, Amsterdam, 1981), and references therein.
[12]M. J. Delaney and S. Ushioda, in *Physics of Superionic Conductors,* edited by M. B. Salamon (Springer-Verlag, Berlin, 1979), pp. 111–139, and references therein.
[13]R. Alben and G. Burns, Phys. Rev. B **16**, 3746 (1977).
[14]M. Falk, and D. Knop, in *Water, a Comprehensive Treatise,* edited by F. Franks (Plenum, New York, 1973), Vol. 2, pp. 55–113, and references therein.
[15]We have used the Program d 506 MINUIT, CERN Program Library.
[16]R. M. Corn and H. L. Strauss, J. Chem. Phys. **76**, 4834 (1982).
[17]G. Brink and M. Falk, Can. J. Chem. **49**, 347 (1971).
[18]S. K. Satija and C. W. Wang, J. Chem. Phys. **68**, 4612 (1978).
[19]G. I. Szàsz, K. Heinzinger, and W. O. Riede, Z. Naturforsch. **36a**, 1067 (1981).
[20]K. Heinzinger, Physica **31B**, 195 (1985).
[21]R. M. Lawrence and R. F. Krush, J. Chem. Phys. **47**, 4758 (1967); see also T. Radnai, G. Patinkas, G. I. Szasz, and K. Heinzinger, Z. Naturforsch. **36a**, 1076 (1981).
[22]G. I. Szasz and K. Heinzinger, J. Chem. Phys. **79**, 3467 (1983).
[23]H. Kanno and J. Hirashi, Chem. Phys. Lett. **72**, 541 (1980).
[24]H. Kanno and J. Hirashi, Phys. Chem. **87**, 3664 (1983).